Published May 25, 2017

Vegetation Indices for Discrimination of Soybean Areas: A New Approach

Carlos Antonio da Silva Junior,* Marcos Rafael Nanni, Paulo Eduardo Teodoro, and Guilherme Fernando Capristo Silva

ABSTRACT

The aim of this study was to map areas cultivated with soybean [*Glycine max* (L.) Merr.] in Paraná state, Brazil, using mono- and multitemporal MODerate-resolution imaging spectroradiometer (MODIS) images. We applied the vegetation index perpendicular crop enhancement index (PCEI) and threshold determination for the automation of soybean area discrimination by geo-object (GEOBIA). For this mapping, vegetation indices (normalized difference vegetation index [NDVI], enhanced vegetation index [EVI], and crop enhancement index [CEI]) and the development of the PCEI were used with the aid of time-series images from the TERRA/MODIS system-sensor. A support analysis, based on geo-objects and a decision tree based on data mining, was used to determine the new vegetation index. "Classification" and "merge region" algorithms and feature extraction were used for classification. To evaluate the precision of the classifications, the Kappa (κ) and overall accuracy (OA) parameters were applied. Regarding the ground line, R and R^2 were above 0.92 and 0.84, respectively ($p < 0.01$). The test results indicate that the proposed methodology is efficient for mapping soybean distribution, with 0.80 for the Kappa parameter, an appropriate crop spatial distribution, and no over- or underestimation of areas. Thus, this study allows automated mapping of areas cultivated with soybean crops at large scales.

Core Ideas

- Automation of mapping of soybean areas.
- Use of remote sensors in the recognition of summer crop.
- Development of exclusive vegetation index for soybean.

Remote sensing is an advanced technology that has been constantly improved, mainly with regard to its application to agriculture. Through this technique, it is possible to determine several crop characteristics, such as leaf area index, estimating areas, production, vegetative vigor, and management (Pan et al., 2012; Peng and Gitelson 2012; da Silva Junior et al., 2016).

In Brazil, despite the improvements with respect to technological knowledge, agricultural areas are often estimated in loco. One of the greatest difficulties in estimating these areas by means of low spatial resolution images is that mixed pixels do not correspond to a unique crop, mainly for small cultivated areas (named "small farmers"), thus hindering classification and requiring additional information from the field and/or provided by the same professionals (Wu and Li 2012).

For agricultural areas with larger spatial extent, the identification problem is minimized with regard to coarse spatial resolution images and different crop phenological stages, which can be spectrally differentiated through multitemporal images (Potgieter et al., 2010). Thus, it is essential to know the agricultural calendar of each crop according to agricultural zoning for a growing region.

The MODIS sensor, on board the TERRA and AQUA satellites, is very useful for mapping large agricultural areas (Ozdogan 2010; Wu and Li 2012; Peng and Gitelson 2012). One of the significant features of its operation is that it provides temporal resolution almost daily (a positive point in obtaining cloud-free images), and image production is with 12-bit quantization in 36 spectral bands.

With available images arising from remote sensing satellites, the development of studies for identifying and monitoring agricultural crops is growing (Peng et al., 2011; Son et al., 2012). During certain stages of development, agricultural crops present phenological patterns that spectrally distinguish them from other vegetable classes. Therefore, the use of satellite time-series images

C.A. da Silva Junior, Geotechnology Applied in Agriculture and Forest (GAAF), State University of Mato Grosso (UNEMAT), Alta Floresta, Mato Grosso, Brazil; M.R. Nanni and G.F.C. Silva, Department of Agronomy (DAG/PGA), State University of Maringá (UEM), Maringá, Paraná, Brazil; P.E. Teodoro, Federal University of Mato Grosso do Sul (UFMS), Chapadão do Sul, Mato Grosso do Sul, Brazil. Received 4 Jan. 2017. Accepted 21 Feb. 2017. *Corresponding author (carlosjr@unemat.br).

Abbreviations: CEI, crop enhancement index; EVI, enhanced vegetation index; GEOBIA, geo-object; MODIS, MODerate-resolution imaging spectroradiometer ; OA, overall accuracy; PCEI, perpendicular crop enhancement index; PVI, perpendicular vegetation index.

Published in Agron. J. 109:1–13 (2017)
doi:10.2134/agronj2017.01.0003

has gained a positive reputation for identifying agricultural crops (Bernardes et al., 2011). Some methods currently used to estimate soybean areas by remote sensing are presented satisfactorily with principal component analysis (Bernardes et al., 2011), guidance on geo-object (da Silva Junior et al., 2014), vegetation index (Rizzi et al., 2009; Risso et al., 2012), and automatic classification (Adami et al., 2010).

Furthermore, the use of remote sensing to study soybean distribution has been confirmed worldwide and is used for discriminating and quantifying areas (da Silva Junior et al., 2014, 2016), identifying phenological stage (Sakamoto et al., 2010) and estimating yield by chlorophyll content (Peng and Gitelson 2012). To meet new methodological challenges for interpreting high resolution images, development of oriented analysis was necessary not only to verify values represented in gray levels but also to verify object shapes and their neighboring relationships (Schiewe and Tufte 2007).

Thus, to overcome problems due to heterogeneity of pixels and, for example, variability of agricultural crops in images obtained by remote sensing, techniques based on objects have been increasingly used in remote sensing (Blaschke 2010). The basic idea of analysis based on an image's objects (GEOBIA) is segmenting and building a hierarchical network of homogeneous objects that, in the case of crop ratings, chart limits.

The development of systematic mapping of agricultural crops in Brazil is a challenge due to its extent of cultivation and multitude of planted crops. The challenge of systematization, especially with regard to the soybean crop, is relevant to Brazil because a large part of its economy is directed toward this activity, and the extent of the agricultural area is currently inaccurate.

The main aim of this study was to estimate and map areas with soybean crop in the state of Paraná, Brazil, using mono and multi-temporal MODIS images. We develop the vegetation index PCEI and apply threshold determination for the automation of soybean area detection by geo-object oriented analysis (GEOBIA).

MATERIALS AND METHODS

Study Area

The study area comprises the state of Paraná in southern Brazil, located between the geographic coordinates 22°29′ to 26°43′ S and 48°20′ to 54°38′ W (Fig. 1), with a total approximate area of 556,439.812 km^2. The altitude is variable, with 52% of the territory higher than 600 m and only 3% lower than 300 m. Three predominant climate types occur, according to Köppen–Geiger's classification (Alvares et al., 2013): Cfa (subtropical with rainfall well distributed over the year and warm summers), Cfb (subtropical with rainfall well distributed over the year and mild summers), and Cwa (subtropical with warm summers and dry winters, occurring in the extreme Northwest of the State).

In the study area, the soils are characterized, according to the Brazilian classification system (EMBRAPA, 2006), as Oxisols, Ultisols, Inceptisols, and Entisols, with the first representing the largest portion of the region.

Climate conditions and fertile soils in the state of Paraná present capacity for different crops, but the soybean crop stands out. According to official data from Companhia Nacional

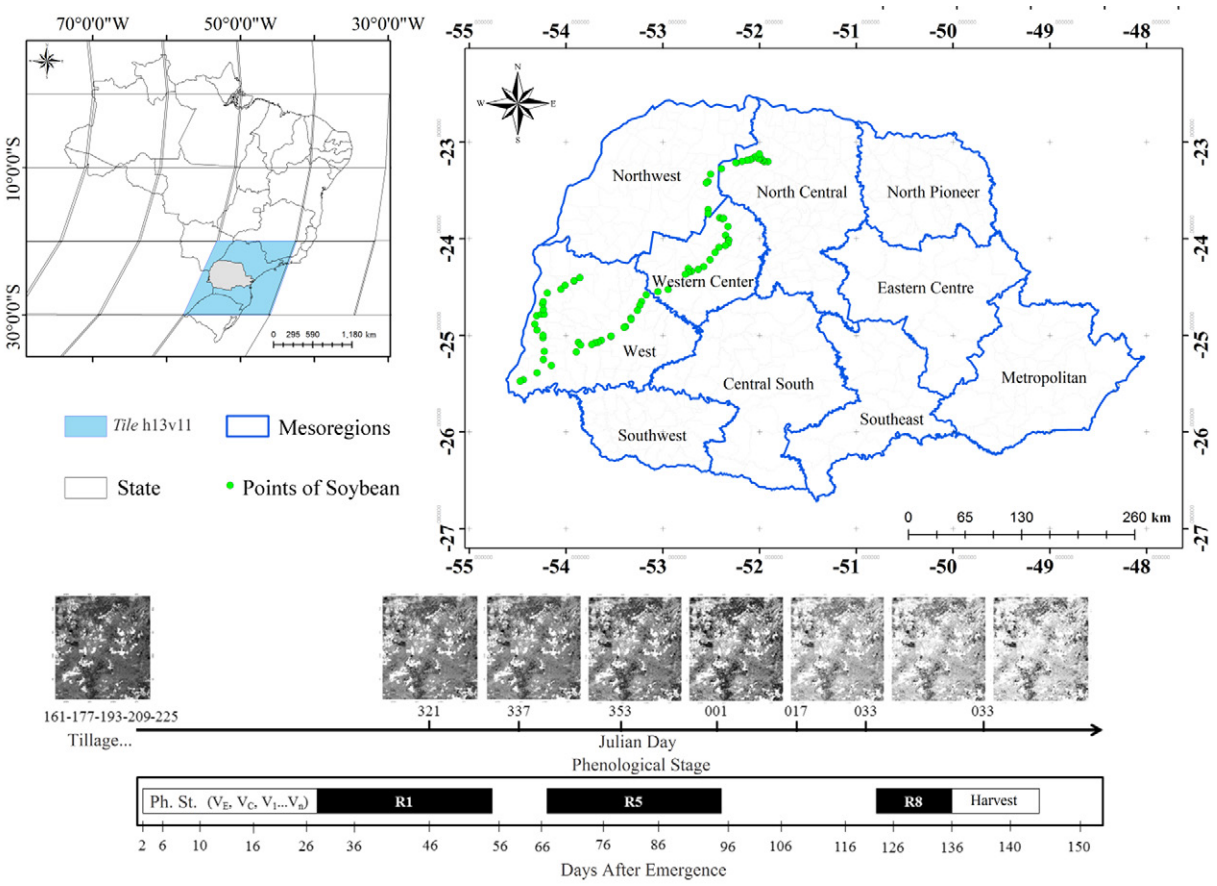

Fig. 1. Top: Location of the study area with its mesoregions, the state of Paraná in southern Brazil. Bottom: Temporal evolution of soybean stages compared to the composition time-series with vegetation indices.

de Abastecimento (CONAB), the state of Paraná contained soybean crop areas for the 2010/2011 harvests of 4,590,500 ha, 2011/2012 of 4,460,600 ha and 2012/2013 of 4,752,800 ha (CONAB, 2011, 2012, 2013).

Because of soybean phenological features, a satellite image acquired on a certain date may contain areas with early or late form planted cultures. In addition, there are areas occupied by sugarcane (*Saccharum* spp.), maize (*Zea mays* L.) in the summer, and oat (*Avena* L.) in the final stages of maturation and harvest. Therefore, the acquisition of multitemporal images is necessary to provide accuracy in soybean area classification.

Summer crops in the study area–rice (*Oryza* spp.), bean (*Phaseolus vulgaris* L.), maize and soybean–are sown from early October to the end of November, while winter crops–oat, sorghum [*Sorghum bicolor* (L.) Moench], and wheat (*Triticum* spp.)–are sown from April to May. Semi-perennial and perennial crops–sugarcane (*Saccharum* spp.), coffee (*Coffea arabica* L.), and citrus (*Citrus* spp.)–as well as pastures and natural vegetation are present all year.

One of the first aspects to be considered in remote mapping of soybean is that its phenology is a progressive process. Therefore, soybean-growing analysis involves the use of a time-series of satellite images. For this study, we selected images with high time resolution to bypass the problems of different sowing times and crop development. This allowed the highlighting of temporal dynamics of the soybean crop, simultaneously providing a distinction from other soil cover classes present at the end of cycle (winter).

Images and Vegetation Indices

We used images from the MODIS sensor, in which the values of the EVI, Eq. [1]) and NDVI of the MOD13Q1 product (http://explorer.usgs.gov), *tile* H13V11, collection 5.0, were established from 16 d MODIS images (Huete et al., 1997) of the TERRA satellite, with spatial resolution of 250 m, downloaded from USGS LP-DAAC.

$$\mathrm{EVI} = g\frac{\rho_{\mathrm{IVP}} - \rho_{\mathrm{V}}}{\rho_{\mathrm{IVP}} + (c_1 \times \rho_{\mathrm{V}}) - (c_2 \times \rho_{\mathrm{A}}) + L} \quad [1]$$

where ρ_{IVP}, ρ_{V}, ρ_{A}, and are the reflectance in the spectral ranges of near infrared (841–876 nm), red (620–670 nm), and blue (459–479 nm), respectively; g is the gain factor (2.5); c_1 and c_2 are the correction coefficients of atmospheric effects for red (6) and blue (7.5), respectively; and $L = 1$ is the correction factor for ground interference.

All images were obtained originally in hierarchical data format (HDF) and sine projection and processed in accordance with the development of batch automation routines (da Silva Junior et al., 2014). Thus, the data are projected to geographic coordinates (latitude and longitude), DATUM WGS-84 (LINZ, 1984) and automatically converted into GeoTIFF format. The dates corresponding to the time-series used are presented in Table 1.

To calculate the CEI, developed by Rizzi et al. (2009), the maximum and minimum values of the EVI for sowing and vegetative growth, respectively, were required. For this, we used the dates corresponding to those in Table 1. The preference of these time intervals was chosen based on the soybean crop calendar in the state of Paraná, in which soil preparation (correction and fertilization) begins in August, the sowing period is between October and November, and desiccation and harvesting proceeds at the end of March.

Table 1. Dates for composing the time-series used, based on time from soil preparation until the final stage of the soybean crop.

Julian Day	Date	Year
161	10 June	2011
177	26 June	2011
193	12 July	2011
209	28 July	2011
225	13 Aug.	2011
321	17 Nov.	2011
337	3 Dec.	2011
353	19 Dec.	2011
001	1 Jan.	2012
017	17 Jan.	2012
033	2 Feb.	2012
049	18 Feb.	2012

Because the soybean crop is at an early stage of its development, part of the reflectance registered by sensor originates from bare ground, which may interfere with values obtained for the CEI. Therefore, we applied the orthogonal vegetation index perpendicular vegetation index (PVI) (Eq. [2]), which cancels the ground reflectance. To implement the PVI, a ground line regression was performed using the spectral bands of red and near infrared, as described by Nanni and Demattê (2006).

$$\mathrm{PVI} = \frac{\rho_{\mathrm{IVP}} - a\rho_{\mathrm{V}} - b}{\sqrt{1 + a^2}} \quad [2]$$

where a and b are, respectively, the slope and intercept of the ground line, which has the ρ_{IVP} band as a dependent variable.

For the development of an index that automatically identifies the soybean crop with a standard threshold slicing, the time-series from preparation to harvest and ground deletion for spectral interference were taken in account. In addition, the full exclusion of the soil by means of ground line or *tasseled cap* avoids the attenuations caused by no-tillage, where the biomass presents in this environment may influence data of vegetation indices mainly with regard to the ratio between bands. In this follow-up, the dates are shown in Table 1, as well as the PVI and its respective maximum and minimum values. With these values, the CEI was improved and renamed PCEI, which is presented by Eq. [3] and synthesized into Eq. [4].

$$\mathrm{PCEI} = g\frac{\left(\mathrm{Max}\frac{\rho_{\mathrm{IVP}} - a\rho_{\mathrm{V}} - b}{\sqrt{1+a^2}} + S\right) - \left(\mathrm{Min}\frac{\rho_{\mathrm{IVP}} - a\rho_{\mathrm{V}} - b}{\sqrt{1+a^2}} + S\right)}{\left(\mathrm{Max}\frac{\rho_{\mathrm{IVP}} - a\rho_{\mathrm{V}} - b}{\sqrt{1+a^2}} + S\right) + \left(\mathrm{Min}\frac{\rho_{\mathrm{IVP}} - a\rho_{\mathrm{V}} - b}{\sqrt{1+a^2}} + S\right)} \quad [3]$$

$$\mathrm{PCEI} = g\frac{(\mathrm{MaxPVI} + S) - (\mathrm{MinPVI} + S)}{(\mathrm{MaxPVI} + S) + (\mathrm{MinPVI} + S)} \quad [4]$$

where MaxPVI is the maximum PVI value observed in the period of maximum development of the soybean crop; MinPVI is the minimum value observed in the pre-sowing and/or emergence period; S is the enhancement coefficient (10^2); and g is the gain factor (10^2).

The CEI and PCEI values range between −1 and 1, which provides a mechanism to verify greater positive differences between maximums and minimums of PVI and EVI observed over the soybean cycle. High values of CEI and PCEI indicate the soybean crop reflectance probability of the pixel. The CEI values were spatialized, creating a numerical map, and subsequently sliced such that values ≥0.28 were considered pixels resulting from soybean and values below this were considered non-soybean sensu Rizzi et al. (2009).

For PCEI values (Eq. [4]), oriented analysis in geo-object was used to indicate polygons in which soybean crops were present. The slicing threshold was defined by data mining. For subsequent confirmation of "soybean" class, stipulated by PCEI, a comparison was performed between terrestrial analyses using soybean reflectance obtained by spectroradiometer and that obtained from MODIS images.

Oriented Analysis and Decision Tree

GEOBIA and data mining and its integration with time-series MODIS images were applied to this analysis. The computing environments (eCognition 8.0- Definiens Developer and Waikato Environment for Knowledge Analysis [WEKA] the platform) for each stage of GEOBIA were added to the data mining approach. eCognition 8.0 is software for image analysis based on objects (Definiens, 2006) developed by Trimble GeoSpatial, while WEKA is equipped with learning algorithms for data mining tasks developed by the University of Waikato, New Zealand (Gao 2009; Hall et al., 2009).

The proposed approach includes the following stages: image segmentation, generation of a training set by selection of polygons, data mining, interpretation, and evaluation of the decision tree, classification of multi-temporal data through decision implementation and validation of the classification. Basic processing units are objects generated by the segmentation algorithm proposed by Baatz and Schäpe (2000) and implemented in the eCognition computer software (Definiens, 2006).

Multi-resolution segmentations were performed using eCognition 8.0, in which the generated objects (polygons) were subjected to the heterogeneity criterion. This criterion can be adjusted by selecting the parameter of scale, weights of spectral bands, form factor, and compactness factor. A range parameter setting, for example, can directly influence the size of generated segments.

To ensure homogeneity of the objects among the four indices utilized (NDVI, EVI, CEI, and PCEI), all images were processed at the same time over the segmentation. A summary of the variables and parameters used in the segmentation are shown in Table 2.

Both classes of objects in the sample, soybean and non-soybean, were selected by checking the reflectance obtained using laboratory remote sensors and the threshold index CEI (≥0.28). In training, 260 objects were selected, of which 130 belonged to the soybean class and 130 to the non-soybean class, which were areas occupied by natural vegetation or other anthropogenic uses.

After the construction of the training set, the eCognition 8.0 platform was used to extract attributes listed in Table 3, which were considered as most representative of the classes of interest. The selected attributes were spectral, spatial, and textural, as described in Blaschke (2010).

In the classification, all child processes were inserted using the *classification* algorithm, where rules are inserted in the proper classes, soybean and non-soybean. After the classification stage, a process with a *merge region* algorithm was inserted. Thus, objects of each class were grouped into larger objects.

Subsequently, after training and evaluating the decision tree, attributes extracted from vegetation indices were classified for mapping areas of soybean and non-soybean for the studied crop years.

The set of rules defined by the attributes and its respective limits identified by the J48 algorithm during data mining stages constitutes the decision tree. The structure of attributes and thresholds was manually implemented by eCognition 8.0 (Definiens, 2006). In the computer software, hierarchical classification is then performed according to the set rules of the decision tree, creating a thematic map with two classes of interest, soybean and non-soybean.

An assessment of thematic map quality for the vegetation indices (CEI and PCEI) and GEOBIA with data mining was performed using a set of samples that was independent of those used for building the models. This approach was adopted to permit a complete evaluation among all classification processes available.

Data Analysis

To generate an independent sample set, we traveled through different regions of the state identifying areas that had soybean crops growing during the chosen period of MODIS image evaluation.

A total of 172 crop reference spots were demarcated (Fig. 1). For this, we used a Trimble brand GPS receiver, GeoExplorer 2008 Series model, with L1 carrier and accuracy better than 5 m after data correction.

Non-soybean spots were collected through visual interpretation of time-series MODIS images (Freitas et al., 2011). These 346 spots were distributed throughout the area and were randomly and independently generated. For establishing this set of samples, we applied the analysis established by Congalton and Green (2009), being the set considered satisfactory for analysis.

Table 2. Summary of variables and parameters used in segmentation.

Segmentation variables	
Image	Weight
NDVI–Julian Day 17†	1
EVI–Julian Day 17	1
CEI–multitemporal	1
PCEI–multitemporal	1
Scale parameter	
Scale	50
Composition homogeneity criteria	
Form	0.1
Compactness	0.5

† NDVI, normalized difference vegetation index; EVI, enhanced vegetation index; CEI, crop enhancement index; and PCEI, perpendicular crop enhancement index.

The quality of classification was quantitatively assessed using the OA coefficients and κ parameter (Eq. [5] and [6], respectively); both were extracted from a confusion matrix (Congalton and Green 2009). In addition, we extracted errors and accuracy under the points of view of the producer and the user (Antunes et al., 2012). These metrics provide a better assessment of the final classification of soybean areas.

$$OA = \left(\frac{\sum_{i=1}^{k} x_{ii}}{N} \right) \quad [5]$$

$$\kappa = \frac{N\sum_{i=1}^{k} x_{ii} - \sum_{i=1}^{k} (x_{i+} \times x_{+i})}{N^2 - \sum_{i=1}^{k} (x_{i+} \times x_{+i})} \quad [6]$$

where κ is the Kappa parameter value; k is the number of lines; x_{ii} is the number of observations in the line i and column i; $\sum_{i=1}^{k} x_{ii}$ is the sum of matrix elements in its main diagonal; x_{i+} is the total sum of observations for lines; x_{+i} is the total sum of observations for columns; and N is the total number of observations.

Having values under the hypothesis of equality between two accuracy coefficients generated from different classifications ($\kappa_1 = \kappa_2$), statistics test were performed using Eq. [7], [8], and [9].

$$Z = \frac{(\hat{\kappa}_1 - \hat{\kappa}_2) - (\kappa_1 - \kappa_2)}{\sqrt{\sigma^2(\hat{\kappa}_1) + \sigma^2(\hat{\kappa}_2)}} \sim N(0,1) \quad [7]$$

$$Z = \frac{\hat{\kappa} - \kappa}{\sqrt{\sigma^2(\hat{\kappa})}} \sim N(0,1) \quad [8]$$

$$\sigma^2(\hat{\kappa}) = \frac{1}{n}\left[\frac{\theta_1(1-\theta_1)}{(1-\theta_2)^2} + \frac{2(1-\theta_1)(2\theta_1\theta_2 - \theta_3)}{(1-\theta_2)^3} + \frac{(1-\theta_1)^2(\theta_4 - 4\theta)_2^2}{(1-\theta_2)^4} \right] \quad [9]$$

where

$$\theta_1 = \frac{\sum_{k=1}^{c} x_{kk}}{n}; \theta_2 = \frac{\sum_{k=1}^{c} x_{k+}x_{+k}}{n^2}; \theta_3 = \frac{\sum_{k=1}^{c} x_{kk}(x_{k+} + x_{+k})}{n^2}; \theta_4 = \frac{\sum_{i=1}^{c}\sum_{j=1}^{c} x_{ij}(x_{i+} + x_{+j})}{n^3}$$

Equality of classifications and the reverse for its differences (H1) were established as the null hypothesis (H0) at the 0.05 significance level ($p < 0.05$).

Finally, the cultivated area estimated by remote sensing was compared to that provided by the Sistema IBGE de Recuperação Automática (SIDRA) from Instituto Brasileiro de Geografia e Estatística (IBGE) to verify the assessment of mapping for the 2011/2012 harvest. Currently, estimates made by IBGE are performed in a subjective way, through interviews with farmers and technicians related to agriculture.

RESULTS AND DISCUSSION

Because the reflectance factor was extracted at various times through MODIS time-series images, ground lines are presented under different forms for the 2011/2012 harvest (Fig. 2). The series with several ground lines is calculated, and then one proceeds with the calculation of the PCEI vegetation index. The diversity of targets presented in a satellite image, especially from the MODIS sensor, showed an extensive imaged band (2330 km), which causes the difference between ground lines. This occurs for the two harvests studied, because at the time of imaging, one could find the following issues: soil tillage, cultivation, and harvesting, as well as other issues that contribute to the spectral response composition received by the sensor, such as forests, urban centers, and various cultures not observed in the line of 45° to the x axis.

Soil can have a strong influence on the determination of a vegetation index, and this influence depends mainly on its spectral properties and type and amount of vegetation present (Galvão and Vitorello 1998). Thus, any type of soil present in the background canopy will contribute negatively to the index for certain vegetation (Gois et al., 2016).

All ground lines obtained and presented by Fig. 2 were built from more than 65,000 random spots of MODIS images only from the state of Paraná. The similarity between them is expected because there were no abrupt, large-scale changes in use and soil occupation during the analyzed time period.

Nanni and Demattê (2006) investigated soil as a direct influence on vegetation index; they obtained the line for different soil classes in a controlled environment. The same authors found R^2 values close to 1.0, that is, almost without data dispersion and alignment of the data on an imaginary abscissa. However, Table 4 shows that for the 2011/2012 harvest, trend equations resulted in high R^2 and were highly significant by t test ($p > 0.01$).

We note that for dates on which summer crops are concentrated, that is, Julian Days 321, 001, 017, 033, and 049, the data trend toward the ground line is spaced and presents as vegetation behavior. This fact was confirmed by trend equations (Table 4); for vegetation in images following Day 321 the R^2 decreases, demonstrating that soil and vegetation are present.

Thus, the angular coefficient values of the trend equations presented in Table 4 for Julian Days 225, 321, and 17 are 1.9310, 2.1764, and 2.5658, respectively. This shows that there is a high probability of the presence of exposed soil on Day 225. With the gradual increase in angular coefficient starting on Day 17, there was full vegetative crop development until its decrease from drying on Day 49, near the time of harvest (angular coefficient 2.6111). In 2011/2012, rainfall occurrences

in the same time period were intense, causing harvest delay, providing greater angular coefficients and a high probability of vegetation presence, thereby confirming the findings of Goulart et al. (2015).

The model for defining soybean in images and acquiring a threshold for the PCEI is presented in the form of a decision tree for the 2011/2012 harvest (Fig. 3).

It is noted that the first branch of the decision tree identified this process by setting a threshold for the PCEI vegetation index (Fig. 3), wherein the average of >0.172464 for values that vary from −1 to 1 can be considered soybean. This threshold was generated by the collection of overlapping samples by the NDVI, EVI, and CEI indices (Rizzi et al., 2009), in which a cut-off threshold of 0.28 was assigned to the last index for soybean.

Table 3. Attributes extracted from eCognition 8.0 for selecting soybean and non-soybean classes.

Type	Name	Values interval features
Spectral	Mean	$\left[C_k^{min}, C_k^{max}\right]$
	Standard deviation	$\left[0, \frac{1}{2} C_k^{range}\right]$
		C_k^{min} : darkest possible intensity value
		C_k^{max} : brightest possible intensity value
Spatial	Area	[0, scene size]
	Asymmetry	[0, 1]
	Border index	[0, ∞], 1 = ideal
	Border length	[0, ∞]
	Compactness	[0, ∞], 1 = ideal
	Density	[0, depended on shaped of image object]
	Length	[0, 1]
	Main direction	[0, 180]
	Rectangular fit	[0, 1],1 = complete fitting, whereas 0 = 0% fit inside the rectangular approximation
	Shape index	[1, ∞] 1 = ideal
Texture	GLCM homogeneity	[0, 90]
	GLCM contrast	[0, 90]
	GLCM dissimilarity	[0, 90]
	GLCM entropy	[0, 90]
Personalized†	NDVI (017)	[−1, 1]
	EVI (017)	[−1, 1]
	CEI	[−1, 1]
	PCEI	[−1, 1]

† NDVI, normalized difference vegetation index; EVI, enhanced vegetation index; CEI, crop enhancement index; and PCEI, perpendicular crop enhancement index.

Table 4. Julian Days from the 2011/2012 harvest, trend equations, coefficient R and R^2 for the relationship between bands of red and near infrared, as obtained by MODIS.

Julian Day	Year	Trend equation	R	R^2
161	2011	$\hat{y} = 2.1700x + 0.1282$	0.95	0.91**
177	2011	$\hat{y} = 2.0449x + 0.1172$	0.94	0.89**
193	2011	$\hat{y} = 1.9607x + 0.1093$	0.94	0.89**
209	2011	$\hat{y} = 1.9533x + 0.1099$	0.93	0.88**
225	2011	$\hat{y} = 1.9310x + 0.1088$	0.93	0.87**
321	2011	$\hat{y} = 2.1764x + 0.1444$	0.92	0.84**
337	2011	$\hat{y} = 2.3036x + 0.1534$	0.92	0.85**
353	2011	$\hat{y} = 2.4553x + 0.1601$	0.94	0.88**
001	2012	$\hat{y} = 2.5267x + 0.1702$	0.93	0.87**
017	2012	$\hat{y} = 2.5658x + 0.1732$	0.93	0.86**
033	2012	$\hat{y} = 2.5959x + 0.1730$	0.94	0.88**
049	2012	$\hat{y} = 2.6111x + 0.1754$	0.94	0.88**

** Significant at 0.01 probability, by t test.

Figure 3 shows that after applying the slicing threshold from PCEI, the soybean crop classification uses the average of CEI index, with a cutoff ≤0.3734. The difficulty in implementing the decision tree using the J48 algorithm was the number of samples collected with appropriate information. Given the "freedom" to execute the algorithm, an extensive and complex tree could result. The consequence of extensive results is replication in the eCognition computer program, which would require costly work and extensive attention.

The attributes chosen by the decision tree for the 2011/2012 harvest (Fig. 3) were average, density, and standard deviation. The decision tree also chose the algorithm CEI and PCEI, which denote suitable discrimination between them in identifying the soybean crop. In this case, the images were generated by mathematical operations (NDVI, EVI, CEI, and PCEI), so the pixel is not a spectral value but a value resulting from an operation. This technique was positive at the time of sample collection because the difference between values was informative at this stage. Thus, as used by the J48 algorithm in the decision tree process, the pixels are statistical, corresponding to the mean and standard deviation in this case.

Different from values obtained in pixel images, texture and color were fundamental in the decision to segment areas such as soybean because spatial distribution could be identified. The texture of targets that correspond to the spatial variation of digital values of the image is one of the features used for identifying targets in an image. Some authors claim that texture is difficult to describe (Marpu 2009). However, the advantages of applying textural information to measure spatial resolution observation data and terrestrial monitoring have been demonstrated in several studies (Dell'Acqua and Gamba 2003; Riedel et al., 2008; da Silva Junior et al., 2014).

Calculating textural metrics using the co-occurrence matrix of the digital value (Gray Level Cooccurrence Matrix-GLCM) shows 14 parameters characteristic of texture (Haralick et al., 1973). This metric extracts texture information using the spatial relationship between digital values for different directions.

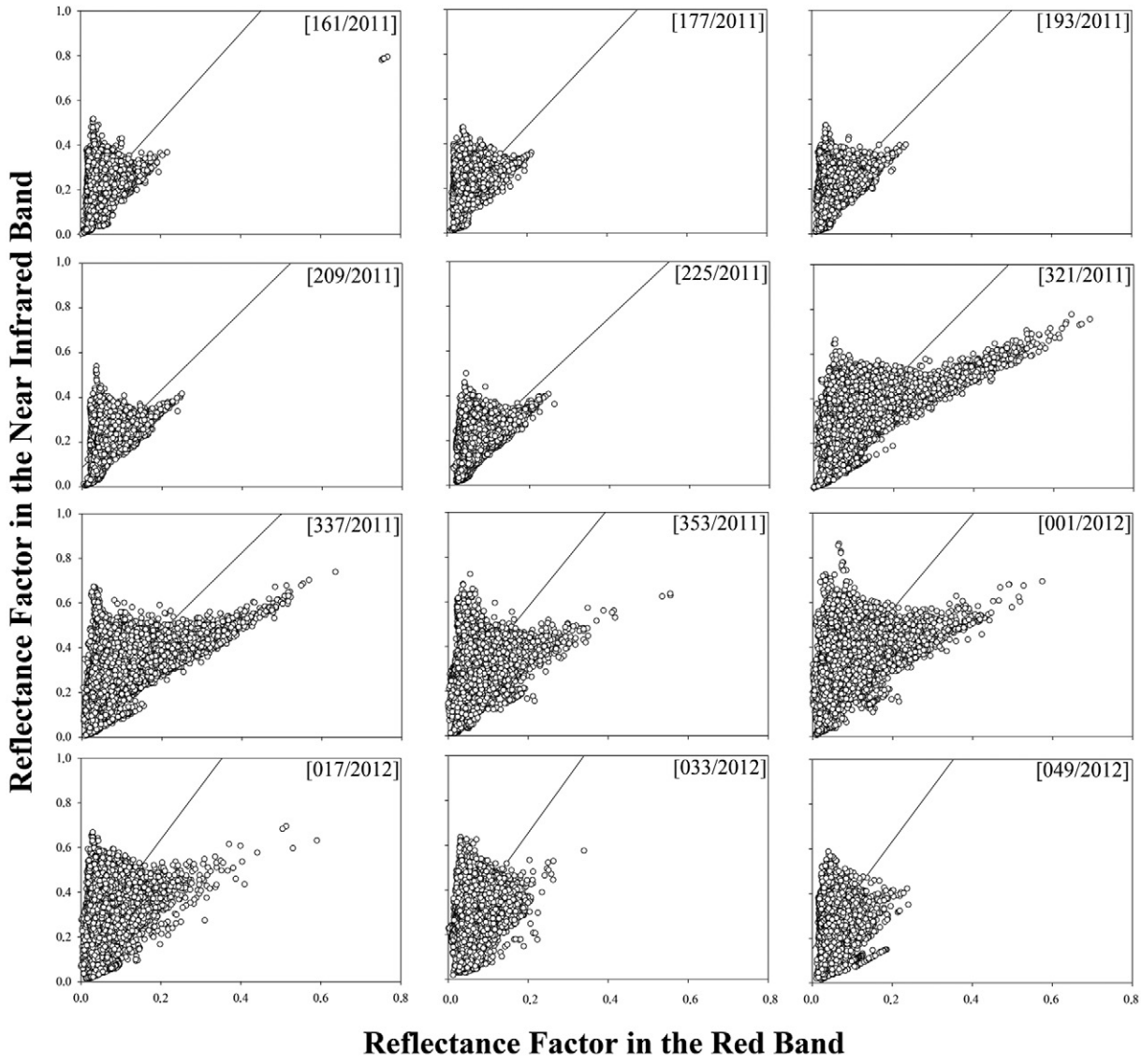

Fig. 2. Ground line obtained from the ratio between bands of red and near infrared using TERRA/MODIS data on the 2011/12 harvest (Julian Days).

Table 5. Confusion matrix of the classifications according to different estimation methods for soybean area and their respective values of Kappa parameter (κ) and overall accuracy (OA) indices for the 2011/2012 harvest.

	Reference			
		CEI†		
Classification	Soybean	Non-soybean	Σ	
Soybean	116	3	119	κ = 0.66
Non-soybean	56	171	227	OA = 0.83
Σ	172	174	346	
		PCEI		
Soybean	131	29	160	κ = 0.59
Non-soybean	41	145	186	OA = 0.80
Σ	172	174	346	
		GEOBIA		
Soybean	72	3	75	κ = 0.40
Non-soybean	100	171	271	OA = 0.70
Σ	172	174	346	

† CEI, crop enhancement index; PCEI, perpendicular crop enhancement index; and GEOBIA, GEOgraphic-object-based image analysis.

Figure 4 presents the correlations between the data obtained from MODIS images for the analyzed harvests and those obtained by spectroradiometer at the greenhouse.

Samples from soybean areas were selected in the MODIS images after processing using the PCEI vegetation index algorithm and correlated with the reflectance values obtained using the FieldSpec 3 for the RGB bands and the NDVI, and EVI.

Because results obtained by regression (R^2) were high and significant by t test ($p < 0.01$), areas indicated by the PCEI present significant potential for such automated mapping. All spectral bands used in the regression were >0.80 except for the NDVI and EVI. The regression was lower when compared to individual bands. This result is possibly due to atmospheric factors not included in the calculations performed at the laboratory level but that were considered at the orbital level.

Higher values are noted when using the spectral images obtained by MODIS because there is no atmospheric interference or scattering by spectroradiometer, thus presenting integer values (Vermote et al., 2002; Yi et al., 2008). In addition, there is a chance that the image would display a spectral mixture in soybean because neighboring interferences can contribute to reflectance, which does not occur in the laboratory.

When analyzing the data obtained using the different methods for estimating soybean areas, we found that the classifications using the PCEI and CEI were highlighted by larger Kappa (κ) and OA parameters. The worsening factor in classifications occurred in GEOBIA for the 2011/2012 harvest (Table 5), which showed the lack of training principle for any object type that was identified.

The κ value shows the conformity of classification obtained. The Kappa parameter has advantages over the OA because it incorporates all elements of the error matrix, whether the objects are correctly classified or not. Furthermore, the κ evaluates thematic accuracy because it is more sensitive to changes

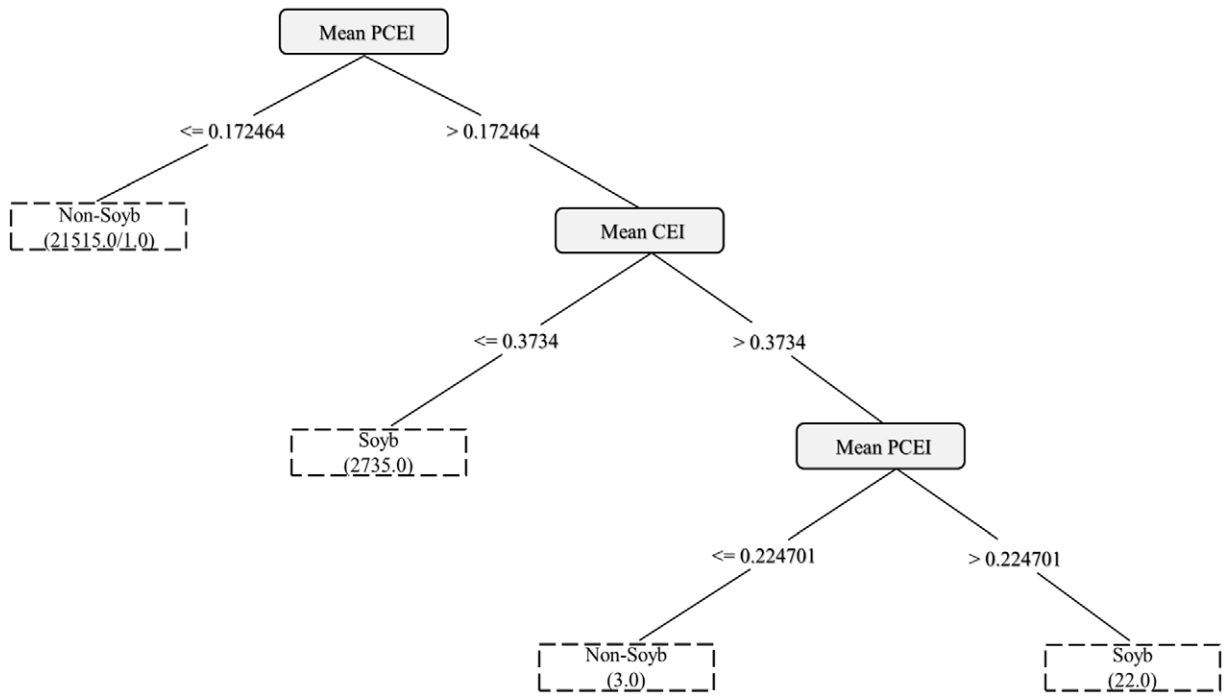

Fig. 3. Decision tree generated by J48 algorithm for the 2011/2012 harvest.

in consumer and producer errors and evaluates the spatial coincidence between two situations (Moreira 2011).

However, regarding the OA parameter, all the adjustments were ≤83% (Table 5), which is below that recommended by Foody (2002), who emphasizes that to reach a satisfactory level, a classification should present an index value above 85%.

The PCEI and GEOBIA methods showed higher values in estimating soybean areas, as observed in Table 5, with Kappa parameters superior to others. In addition, PCEI is present in data mining and is used as the main attribute in the decision tree generated by WEKA 3.6.8. Usually, data mining is the process of data analysis from different perspectives to summarize it into useful information, which is the process of finding correlations or patterns among dozens of related fields in a large database (Yang et al., 2008).

Kappa, which evaluates the agreement or disagreement between classifications, varied between 0.40 (GEOBIA) and 0.66 (CEI–Table 5), which, according to the classification proposed by Landis and Koch (1977), is from reasonably good to good quality ($\kappa > 0.21$ and 0.81), respectively.

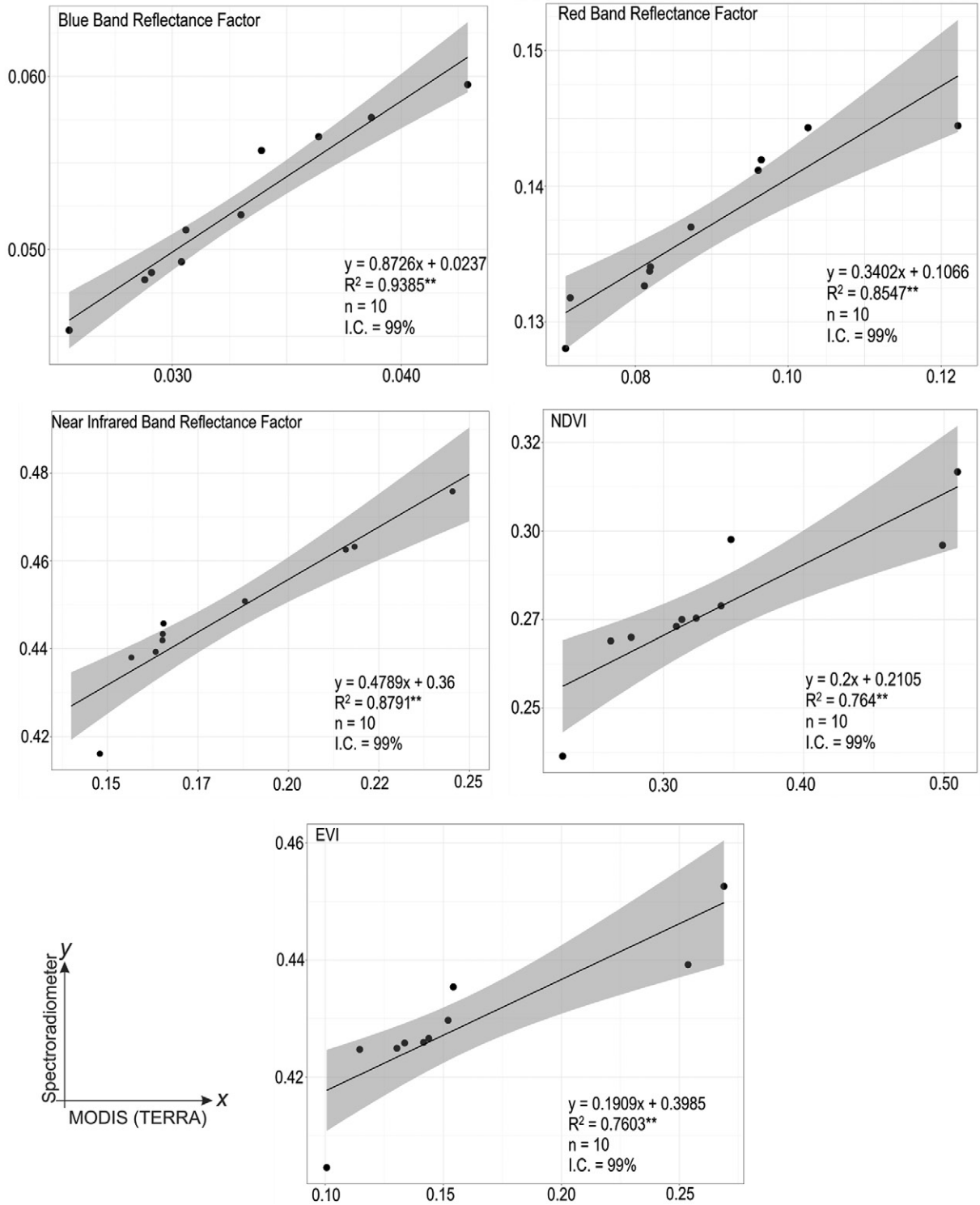

Fig. 4. Simple linear regressions between orbital and terrestrial data for the soybean areas in the 2011/2012 harvest.

Thus, it can be said that thematic maps generated for the soybean crop, especially when CEI is used, approached the official data. The values are also significant compared to studies that used the same sensor but other methods, such as Lamparelli et al. (2008), who estimated soybean areas with MODIS data, obtaining a κ parameter between 0.60 and 0.80.

These results are similar to those obtained by Rudorff et al. (2007) in the state of Rio Grande do Sul when estimating the soybean crop with the MODIS sensor (MOD13Q1 product), where they obtained OA parameters of 76.17% and a κ of 0.50, considered by Pax–Lenney and Woodcock (1997) as good performance.

For measuring the accuracy of each category, soybean and non-soybean, we used the error from the producer's and consumer's point of view for the studied harvests (Tables 6 and 7) by analyzing the inclusion of errors and omission of errors present in the classifications (Antunes et al., 2012).

When analyzing the data from producer and consumer errors–inclusion and omission, respectively–it is noteworthy that the lowest value for the inclusion error for the soybean class was obtained with the classification using the PCEI, with errors from 0.24 to 0.18, while for the same class, the omission errors in this classification were 0.17 and 0.22 (Tables 6 and 7, respectively). This means that 76% of the areas were classified as soybean, while 83% corresponded to the non-soybean class. Thus, the producer error occurs when an object is included in the class to which it does not belong, while the consumer error occurs when an object is removed from the class to which it belongs (Johann et al., 2012).

One of the analytical methods with producer error that should be highlighted for the soybean class was the CEI index (Table 6), with a value of 0.33. However, from the consumer's point of view, the accuracy was 97% for the soybean class and 75% for the non-soybean class. Thus, even with a rating of 67% for the areas identified as soybean, more than 95% of these areas actually had this use, that is, the areas of this class have been appropriately classified, but underestimated.

Table 6. Error and accuracy from the producer's and consumer's point of view for the Error Matrix for the soybean class built from the images.

	Producer		Consumer	
	Error	Accuracy	Error	Accuracy
Analysis method†	2011/2012			
CEI	0.33	0.67	0.03	0.97
PCEI	0.24	0.76	0.18	0.82
GEOBIA	0.58	0.42	0.04	0.96

† CEI, crop enhancement index; PCEI, perpendicular crop enhancement index; and GEOBIA, GEOgraphic-object-based image analysis.

Table 7. Error and accuracy of the producer and consumer's point of view for the Error Matrix for non-soybean class, constituted from the images.

	Producer		Consumer	
	Error	Accuracy	Error	Accuracy
Analysis method†	2011/2012			
CEI	0.02	0.98	0.25	0.75
PCEI	0.17	0.83	0.22	0.78
GEOBIA	0.02	0.98	0.37	0.63

† CEI, crop enhancement index; PCEI, perpendicular crop enhancement index; and GEOBIA, GEOgraphic-object-based image analysis.

On the other hand, the non-soybean class (Table 7) highlights the value obtained in the producer error presented in the GEOBIA method. For the consumer, the same was not observed, since the errors obtained were 0.25, 0.22 and 0.37, having, as a consequence, a higher estimate of the soybean class and a reduction in non-soybean class.

Thus, GEOBIA takes into account different attributes in the context of space in which the targets were inserted from the segmentation process. However, for the non-soybean class, there was a small difference between the errors of GEOBIA and slicing performed in the CEI and PCEI because the contingent of the spectral mixture is greater and more generalized for the classifiers.

Hypothesis tests depending on the results of the products are shown in Table 8. By analyzing the data obtained in estimates of soybean areas, it was verified that some classifications showed equality before the *Z* test for the κ and OA (AG) parameters for the PCEI and CEI.

Through the *Z* test, it was verified that classification by GEOBIA showed lower κ values when compared to PCEI and CEI (Table 8), possibly due to some confusion by the user in training, that is, the selected polygons. This can occur in further application in distinct environments, so great attention is required during polygon collection.

For the parameter κ, most of the tests resulted in a significant difference, except the above-mentioned comparisons. It is noteworthy that the closer to zero the *p* value, the greater the evidence against the hypothesis of equality. This was observed when a comparison among the classifications parameters was performed, in addition to other above-mentioned comparatives that obtained absolute zero.

Table 8. Hypothesis tests to compare the results of accuracy between indices for the 2011/2012 harvest.

$Kappa_1$ vs. $Kappa_2$	Z	*p* value
GEOBIA × CEI†	–4.56	0.0000*
GEOBIA × PCEI	–3.24	0.0006*
CEI × PCEI	1.09	0.1375ns‡

* Significant at 0.05 probability level.

† CEI, crop enhancement index; PCEI, perpendicular crop enhancement index; and GEOBIA, GEOgraphic-object-based image analysis.

‡ ns, not significant.

Table 9. Estimated soybean areas in hectares per mesoregion of the state of Paraná for the 2011/2012 harvest.

Mesoregion	CEI†	PCEI	GEOBIA
Northwest	50,883.02	178,181.12	47,878.88
Western center	149,807.29	378,627.85	180,654.38
North central	199,022.73	577,950.37	270,603.71
North pioneer	59,526.95	282,145.61	77,608.00
East central	137,759.51	563,691.63	134,830.31
West	240,424.91	599,466.51	316,590.17
Southwest	11,129.68	72,349.19	4340.70
Central south	168,700.28	624,842.44	183,489.89
Southeast	73,311.02	438,704.41	57,103.65
Metropolitan	47,747.72	379,839.50	44,187.72
Total	1138,313.11	4,095,798.63	1,317,287.41

† CEI, crop enhancement index; PCEI, perpendicular crop enhancement index; and GEOBIA, GEOgraphic-object-based image analysis.

For the studied municipalities, the results were quantified in hectares of soybean growing per mesoregion, which are presented in Table 9.

When compared to official data (IBGE, 2013), the PCEI technique was comparable to official data. In the analysis performed by the *Z* test, it was observed using the technique here that all values were significant at 95% probability and were superior when compared with other κ parameters generated by other classifications. This result demonstrates that estimates are similar to official data.

Soybean areas estimated by Table 9 show similarity between the classifications performed by PCEI and those estimated by official data (IBGE, 2013). In terms of the CEI index showing a better κ parameter, as presented in Table 5 and confirmed in Table 8, it underestimated the values when used in a principal component analysis (da Silva Junior et al., 2015).

It is emphasized that these estimates are based on objective (statistical) methods using satellite images with a spatial resolution of 250 m, compared to estimates of SIDRA/IBGE, which are obtained subjectively through interviews with producers, meetings with technicians for planting intention verification, and crops sold.

However, objective methods also carry uncertainties, being confirmed only with reliable data that are represented in reality. Normally, there are over- or underestimates when compared to official data, as also observed by Xiao et al. (2010), Ippoliti-Ramilo et al. (2003), Lamparelli et al. (2008), Ozdogan (2010), Pan et al. (2012), Peng and Gitelson 2012), Wu and Li (2012), who work with remote sensing techniques in the estimation of agricultural areas.

Figure 5 shows the spatial distribution of soybean in the state of Paraná (Brazil) obtained by different classification systems. By observing the distribution of soybean classes, we note the similarity between areas in the classification using the CEI and GEOBIA indices.

Classifiers that underestimated the areas (Table 9) were of lower color intensity than the estimates of possible soybean areas. The methodological techniques demonstrated and assessed here present significant potential for soybean mapping, thus having the potential for use as a complement to official state and federal agencies in crop management, specializing in details by municipality and obtaining faster objective agricultural statistics. As shown in Fig. 6, there is a general similarity between the spatial distributions from the estimates of soybean areas and the classification with the PCEI.

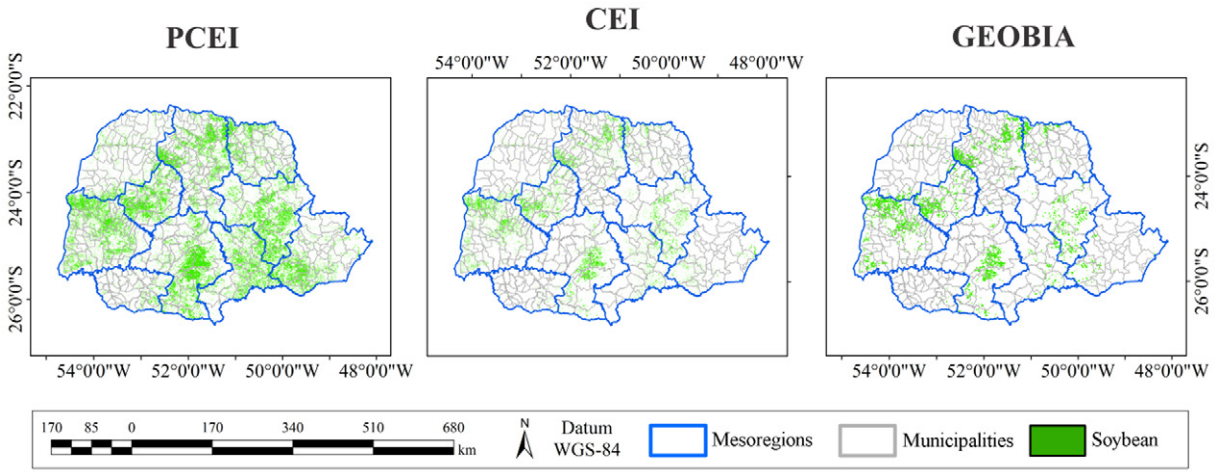

Fig. 5. Spatial distribution of soybean-growing areas in the 2010/2011 harvest, according to various classification techniques.

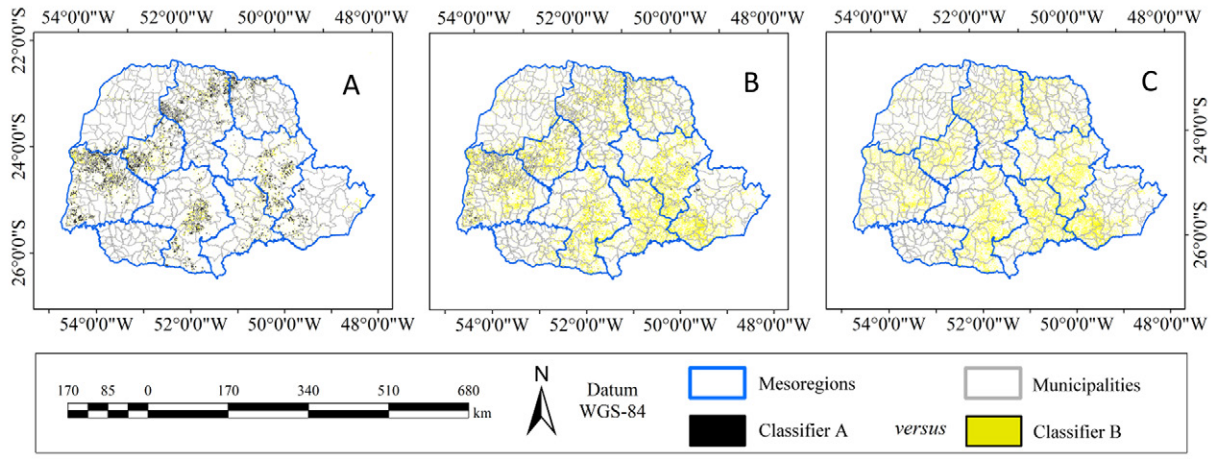

Fig. 6. Maps of the differences between the classifications performed by GEOBIA × CEI, GEOBIA × PCEI and CEI × PCEI (A, B and C, respectively).

CONCLUSIONS

The mapping, discrimination and quantification of soybean areas in the state of Paraná, Brazil, is possible with the use of MODIS classifiers and images, in which the systematization presented satisfactory results based on the κ, OA parameters, and the regression and concordance coefficients in the period of study.

The development of the PCEI obtained satisfactory results in comparison to other vegetation indices used in the literature, mainly when minimizing soil reflectance supported by time-series, with a cutting threshold of 0.172464 obtained by means of a decision tree. Thus, values higher than this threshold represent the soybean crop when composing the images proposed here. This new approach can be routinely used by soybean producers.

ACKNOWLDEGMENTS

We thank: Brazilian Council for Scientific and Technological Development (CNPq), Financier of Studies and Projects (FINEP), and the Coordination for the Upgrading of Higher Education Personnel (CAPES) for their grants and funding; reviewers and editors for their valuable comments and contributions to improve the manuscript; and "*Assessoria de Gestão de Pesquisa e Pós-Graduação*" of UNEMAT, Campus of Alta Floresta, for the valuable suggestions to improve the text.

REFERENCES

Adami, M., R. Rizzi, M.A. Moreira, B.F.T. Rudorff, and C.C. Ferreira. 2010. Amostragem probabilística estratificada por pontos para estimar a área cultivada com soja. Pesqi. Agropecu. Bras. 45:585–592.

Alvares, C.A., J.L. Stape, P.C. Sentelhas, J.L. De Moraes Goncalves, and G. Sparovek. 2013. Koppen's climate classification map for Brazil. Meteorol. Z. 22:711–728. doi:10.1127/0941-2948/2013/0507

Antunes, J.F.G., E. Mercante, J.C.D.M. Esquerdo, R.A. Lamparelli, and J.V. Rocha. 2012. Estimativa de área de soja por classificação de imagens normalizada pela matriz de erros. Pesqi. Agropecu. Bras. 47:1288–1294. doi:10.1590/S0100-204X2012000900014

Baatz, M., and A. Schäpe. 2000. Multiresolution segmentation–An optimization approach for high quality multi-scale image segmentation. In: J. Strobl and T. Blaschke , editors, Angewandte Geographische Informationsverarbeitung XII. Beiträge zum AGIT Symposium Salzburg 2000. Karlsruhe. Herbert Wichmann Verlag. Int. Trade Ctr., Enschede, the Netherlands. p. 12–23.

Bernardes, T., M. Adami, A.R. Formaggio, M.A. Moreira, D.A. França, and M.R. Novaes. 2011. Imagens mono e multitemporais Modis para estimativa da área com soja no Estado de Mato Grosso. Pesqi. Agropecu. Bras. 46:1530–1537. doi:10.1590/S0100-204X2011001100015

Blaschke, T. 2010. Object based image analysis for remote sensing. ISPRS J. Photogramm. Remote Sens. 65:2–16. doi:10.1016/j.isprsjprs.2009.06.004

CONAB. 2011. Acompanhamento de safra brasileira: Grãos, décimo segundo levantamento, setembro 2011. Compania Nacional de Abastecimento. http://www.conab.gov.br/OlalaCMS/uploads/arquivos/11_09_19_09_49_47_boletim_setembro-2011.pdf (accessed 20 Nov. 2013).

CONAB. 2012. Acompanhamento de safra brasileira: Grãos, décimo segundo levantamento, setembro 2012. Compania Nacional de Abastecimento. http://www.conab.gov.br/OlalaCMS/uploads/arquivos/12_09_06_09_18_33_boletim_graos_-_setembro_2012.pdf (accessed 20 Nov. 2013).

CONAB. 2013. Acompanhamento de safra brasileira: Grãos, décimo segundo levantamento, setembro 2013. Compania Nacional de Abastecimento. http://www.conab.gov.br/OlalaCMS/uploads/arquivos/13_10_16_14_32_01_boletim_portugues_-_setembro_2013.pdf (accessed 20 Nov. 2013).

Congalton, R.G., and K. Green. 2009. Assessing the accuracy of remotely sensed data: Principles and practices. 2nd ed. CRC Press, Boca Raton, FL.

da Silva Junior, C.A., T. Frank, and T.C.S. Rodrigues. 2014. Discriminação de áreas de soja por meio de imagens EVI/MODIS e análise baseada em geo-objeto. Rev. Bras. Eng. Agríc. AMB (Sao. Paulo) 18:44–53.

da Silva Junior, C.A., M.R. Nanni, E. Cezar, A.C. Gasparotto, A.A. Silva, G.F.C. Silva et al. 2015. Principal component analysis in monitoring soybean fields of Brazil through the MODIS sensor. J. Agron. 14:72–79.

da Silva Junior, C.A., M.R. Nanni, P.E. Teodoro, G.F.C. Silva, M.G. Lima, and M. Eri. 2016. Comparison of mapping soybean areas in Brazil through perceptron neural networks and vegetation indices. African J. Agric. Res. 11:114413–114424.

Definiens. 2006. Definiens professional 5: Reference book. The Imaging Intelligence Company, Munich, Germany.

Dell'Acqua, F.P., and P. Gamba. 2003. Texture-based characterization of urban environments on satellite SAR images. IEEE Trans. Geosci. Rem. Sens. 41:153–159. doi:10.1109/TGRS.2002.807754

EMBRAPA. 2006. Sistema brasileiro de classificação de solos. 2nd ed. Embrapa Produção de Informação, Brasília. Embrapa Solos, Rio de Janeiro.

Foody, G.M. 2002. Status of land cover classification accuracy assessment. Remote Sens. Environ. 80:185–201. doi:10.1016/S0034-4257(01)00295-4

Freitas, R.M., E. Arai, M. Adami, A.F. Souza, F.Y. Sato, Y.E. Shimabukuro et al. 2011. Virtual laboratory of remote sensing time series: Visualization of MODIS EVI2 data set over South America. J. Comp. Interdis. Sci. 2:57–68.

Galvão, L.S., and Í. Vitorello. 1998. Variability of laboratory measured soil lines of soil from southeastern Brazil. Remote Sens. Environ. 63:166–181. doi:10.1016/S0034-4257(97)00135-1

Gao, J. 2009. Digital analysis of remotely sensed imagery. McGraw-Hill Professional, Maidenhead, UK .

Gois, G., R.C. Delgado, J.F. Oliveira-Júnior, P.E. Teodoro, and T.C.O. Souza. 2016. EVI2 Index trend applied to the vegetation of the State of Rio de Janeiro based on non-parametric tests and Markov chain. Biosci. J. 32:1049–1058. doi:10.14393/BJ-v32n4a2016-33713

Goulart, A.C.O., R.C. Delgado, J.F. Oliveira-Júnior, G. Gois, and E.S. Oliveira. 2015. Vegetation indexes and rain time-spectrum relationship in the city of Rio de Janeiro. R. Ciênc. Agr. 58:277–283.

Hall, M., E. Frank, G. Holmes, B. Pfahringer, P. Reutemann, and I. Witten. 2009. The WEKA data mining software: An update. ACM SIGKDD Explor. Newslet. 11:10–18. doi:10.1145/1656274.1656278

Haralick, R.M., K. Shanmugam, and I. Dinstein. 1973. Textural features for image classification. IEEE Trans. Sys. Man and Cyber. SMC-3:610–621. doi:10.1109/TSMC.1973.4309314

Huete, A.R., H.Q. Liu, K. Batchily, and W.V. Leeuwen. 1997. A comparison of vegetation indices over a global set of TM images for EOS-MODIS. Remote Sens. Environ. 59:440–451. doi:10.1016/S0034-4257(96)00112-5

IBGE. 2013. SIDRA–Sistema IBGE de Recuperação Automática. Inst. Brasileiro de Geografia e Estatistica. http://www.sidra.ibge.gov.br (accessed 2 Oct. 2013).

Ippoliti-Ramilo, G., J.C.N. Epiphanio, and Y.E. Shimabukuro. 2003. Landsat-5 thematic mapper data for pre-planting crop area evaluation in tropical countries. Int. J. Remote Sens. 24:1521–1534. doi:10.1080/01431160010007105

Johann, J.A., J.V. Rocha, D.G. Duft, and R.A.C. Lamparelli. 2012. Estimativa de áreas com culturas de verão no Paraná, por meio de imagens multitemporais EVI/Modis. Pesqi. Agropecu. Bras. 47:1295–1306. doi:10.1590/S0100-204X2012000900015

Lamparelli, R.A.C., M.O.C. Waste, and E. Marcante. 2008. Mapeamento de semeaduras de soja (*Glycine max* (L.) Merr.) mediante dados MODIS/Terra e TM/Landsat 5: Um comparativo. Eng. Agric. 28:334–344.

Landis, J.R., and G.G. Koch. 1977. The measurement of observer agreement for categorical data. Biometrics 33:159–174.

LINZ (Land Information New Zealand). 1984. World Geodetic System. http://www.linz.govt.nz/data/geodetic-system/datums-projections-and-heights/geodetic-datums/world-geodetic-system-1984-wgs84 (accessed 1 May 2017). LINZ, Wellington, New Zealand.

Marpu, P.R. 2009. Geographic object-based image analysis. Freiberg, 121f. Ph.D. thesis. Engineering-Faculty of Geosciences, Geo-Engineering and Mining Technische Universität Bergakademie Freiberg.

Moreira, M.A. 2011. Fundamentos do Sensoriamento Remoto e metodologias de Aplicação. 4th ed. Editora UFV, Viçosa.

Nanni, M.R., and J.A.M. Demattê. 2006. Comportamento da linha do solo obtida por espectrorradiometria laboratorial para diferentes classes de solo. Rev. Bras. Cienc. Solo 30:1031–1038. doi:10.1590/S0100-06832006000600012

Ozdogan, M. 2010. The spatial distribution of crop types from MODIS data: Temporal unmixing using Independent Component Analysis. Remote Sens. Environ. 114:1190–1204. doi:10.1016/j.rse.2010.01.006

Pan, Y., L. Li, J. Zhang, S. Liang, X. Zhu, and D. Sulla-Menashe. 2012. Winter wheat area estimation from MODIS-EVI time series data using the crop proportion phenology index. Remote Sens. Environ. 119:232–242. doi:10.1016/j.rse.2011.10.011

Pax-Lenney, M., and C.E. Woodcock. 1997. The effect of spatial resolution on the ability to monitor the status of agricultural lands. Remote Sens. Environ. 61:210–220. doi:10.1016/S0034-4257(97)00003-5

Peng, Y., and A.A. Gitelson. 2012. Remote estimation of gross primary productivity in soybean and maize based on total crop chlorophyll content. Remote Sens. Environ. 117:440–448. doi:10.1016/j.rse.2011.10.021

Peng, D., A.R. Huete, J. Huang, F. Wang, and H. Sun. 2011. Detection and estimation of mixed paddy rice cropping patterns with MODIS data. Int. J. Appl. Earth Obs. Geoinf. 13:13–23. doi:10.1016/j.jag.2010.06.001

Potgieter, A.B., A. Apan, G. Hammer, and P. Dunn. 2010. Early-season crop area estimates for winter crops in NE Australia using MODIS satellite imagery. ISPRS J. Photogramm. Remote Sens. 65:380–387. doi:10.1016/j.isprsjprs.2010.04.004

Riedel, T., C. Thiel, and C. Schmullius. 2008. Fusion of multispectral optical and SAR images towards operational land cover mapping in Central Europe. In: T. Blaschke, S. Lang, and G.J. Hay, editors, Object-based Iimage analysis spatial concepts for knowledge-driven remote sensing applications. Springer, Berlin, Germany. p. 493–511. doi:10.1007/978-3-540-77058-9_27

Risso, J., R. Rizzi, B.F.T. Rudorff, M. Adami, Y.E. Shimabukuro, A.R. Formaggio, and R.D.V. Epiphanio. 2012. Índices de vegetação Modis aplicados na discriminação de áreas de soja. Pesqi. Agropecu. Bras. 47:1317–1326. doi:10.1590/S0100-204X2012000900017

Rizzi, R., J. Risso, R.D.V. Epiphanio, B.F.T. Rudorff, A.R. Formaggio, Y.E. Shimabukuro, and S.L. Fernandes. 2009. Estimativa da área de soja no Mato Grosso por meio de imagens MODIS. In: Proceedings of the 14th Brazilian Remote Sensing Symposium, Natal, RN, Brazil. 25–30 Apr. 2009. INPE, São José dos Campos, SP, Brazil. p. 387–394.

Rudorff, C.M., R. Rizzi, B.F.T. Rudorff, L.M. Sugawara, and C.A.O. Vieira. 2007. Spectral-temporal response surface of MODIS sensor images for soybean area classification in Rio Grande do Sul State. Cienc. Rural 37:118–125. doi:10.1590/S0103-84782007000100019

Sakamoto, T., D. Brian, B.D. Wardlowa, A.A. Gitelson, S.B. Verma, A.E. Suyker, and T.J. Arkebauer. 2010. A two-step filtering approach for detecting maize and soybean phenology with time-series MODIS data. Remote Sens. Environ. 114:2146–2159. doi:10.1016/j.rse.2010.04.019

Schiewe, J., and L. Tufte. 2007. O potencial de procedimentos baseados em regiões para a avaliação integrada de dados de SIG e sensoriamento remoto. In: T. Blaschke and H. Kux, organizers, Sensoriamento remoto e SIG avançados. Editora Oficina de Textos, São Paulo. p. 56–65.

Son, N.T., C.F. Chen, C.R. Chen, L.Y. Chang, and V.Q. Minh. 2012. Monitoring agricultural drought in the Lower Mekong Basin using MODIS NDVI and land surface temperature data. Int. J. Appl. Earth Obs. Geoinf. 18:417–427. doi:10.1016/j.jag.2012.03.014

Vermote, E.F., N.Z. El Saleous, and C.O. Justice. 2002. Atmospheric correction of MODIS data in the visible to middle infrared: First results. Remote Sens. Environ. 83:97–111. doi:10.1016/S0034-4257(02)00089-5

Wu, B., and Q. Li. 2012. Crop planting and type proportion method for crop acreage estimation of complex agricultural landscapes. Int. J. Appl. Earth Obs. Geoinf. 16:101–112. doi:10.1016/j.jag.2011.12.006

Xiao, X., S. Boles, S. Frolking, W. Salas, B. Moore, C. Li, L. He, and R. Zhao. 2010. Landscape-scale characterization of cropland in China using Vegetation sensor data and Landsat TM imagery. Int. J. Remote Sens. 23:3579–3594. doi:10.1080/01431160110106069

Yang, T.L., P. Bai, and Y.S. Gong. 2008. Spatial Data Mining Features between general Data Mining. Inter. Works. ETT and GRS 2:541–544.

Yi, Y., D. Yang, J. Huang, and D. Chen. 2008. Evaluation of MODIS surface reflectance products for wheat leaf area index (LAI) retrieval. Remote Sens. Environ. 63:661–677.